Supporting Information

Ni_3S_2/Co_3S_4 with controlled surface electron arrangement for high-performance aqueous energy storage

Miaomiao Liang[a], Zhenyang Li[a], Yongxia Kang[a], Xiaoliang Zhao[a], Xiaozhe Zhang[a], Hemeng Zhang[a], Haiyang Wang[b,*], Zongcheng Miao[b,c,*], Chong Fu[a,*]

[a]School of Materials Science and Engineering, Xi'an Key Laboratory of Textile Composites, Xi'an Polytechnic University, Xi'an, 710048, China

[b]School of Artificial Intelligence, Optics and Electronics (iOPEN), Northwestern Polytechnical University, Xi'an, 710072, Shaanxi, China

[c]Technological Institute of Materials & Energy Science (TIMES), Xi'an Key Laboratory of Advanced Photo-electronics Materials and Energy Conversion Device, Xijing University, Xi'an, 710123, China

E-mail addresses: why0224@126.com; miaozongcheng@nwpu.edu.cn; fuchong69@163.com

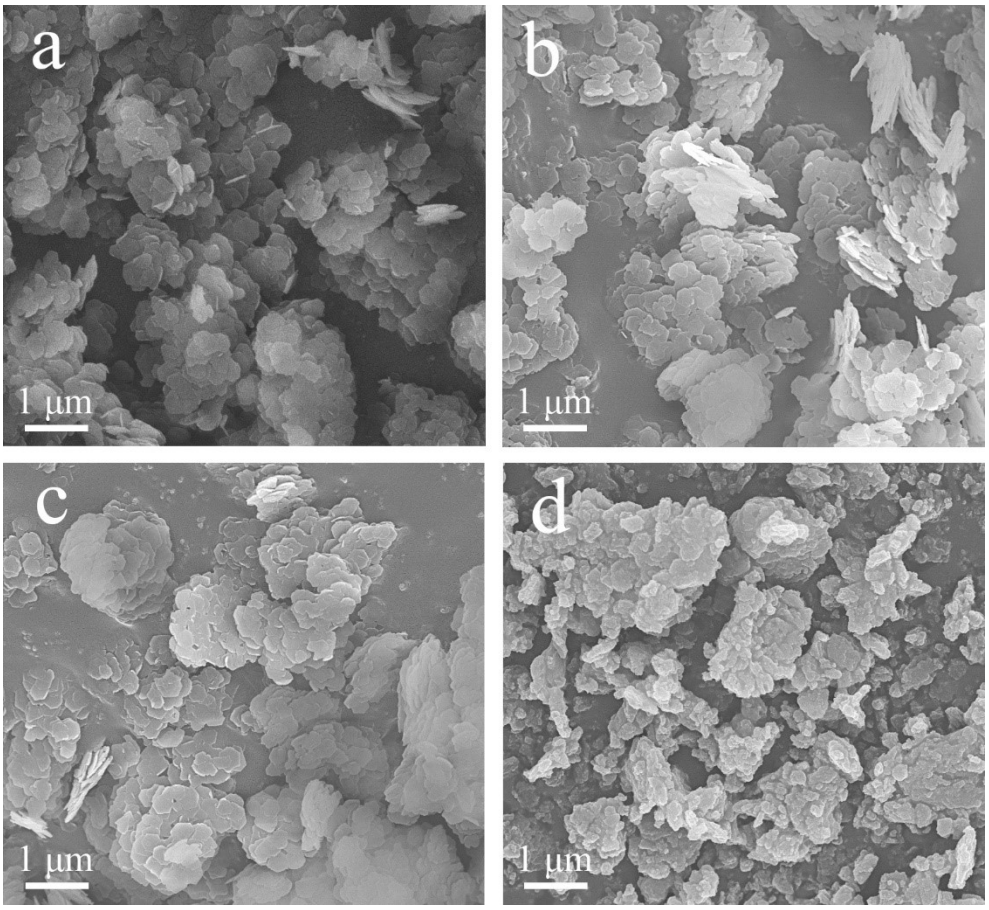

Fig. S1 SEM images of (a) $Co_5(O_{9.48}H_{8.52})NO_3$, (b) $Ni/Co_5(O_{9.48}H_{8.52})NO_3$, (c) Ni_3S_2/Co_3S_4, (d) Ni_3S_2/Co_3S_4-Sv, respectively under low magnifications.

Table S1 The specific ICP results of Ni_3S_2/Co_3S_4-Sv sample

Sample Name	Mass m_0 (g)	Constant Volume V_0 (mL)	Test Element	Concentration of tested element in solution C_0 (mg/L)	Dilution factor f	Element concentration in original decomposition reagent C_1 (mg/L)	Element Content C_x (mg/kg)	Average Value (mg/kg)	%
Ni_3S_4/Co_3S_4-Sv	0.02070	50	Co	4.3564	50	217.82000	526135.27	5.23E+05	52.3%
	0.02045	50		4.2597	50	212.98500	520745.72		
	0.02070	50	Ni	1.9571	10	19.57100	47272.95	4.69E+04	4.69%
	0.02045	50		1.8997	10	18.99700	46447.43		

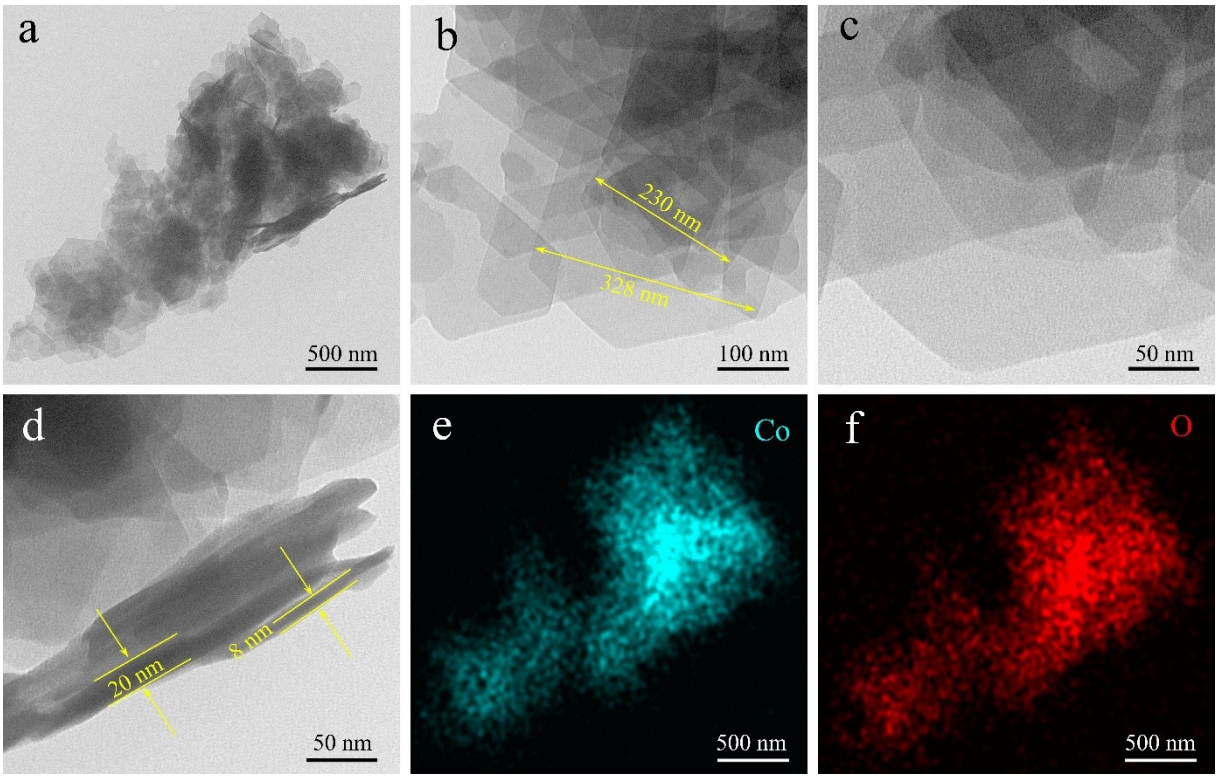

Fig. S2 (a), (b), (c), (d) TEM and elemental mapping of (e) Co, (f) O in $Co_5(O_{9.48}H_{8.52})NO_3$

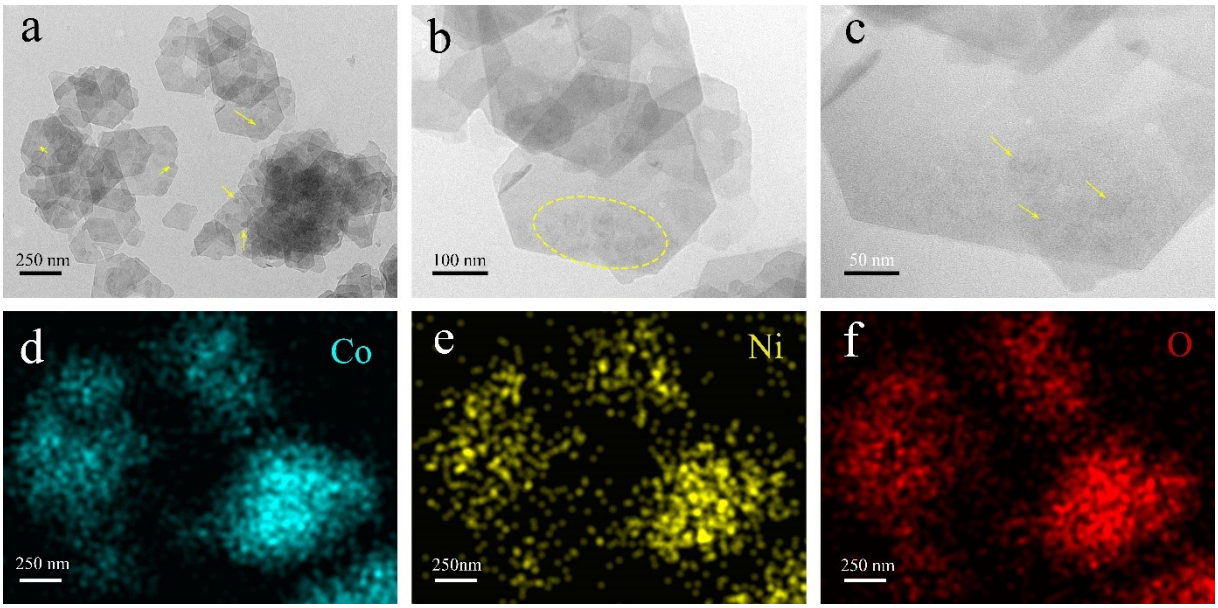

Fig. S3 (a), (b), (c) TEM and elemental mapping of (d) Co, (e) Ni, (f) O in

$Ni/Co_5(O_{9.48}H_{8.52})NO_3$

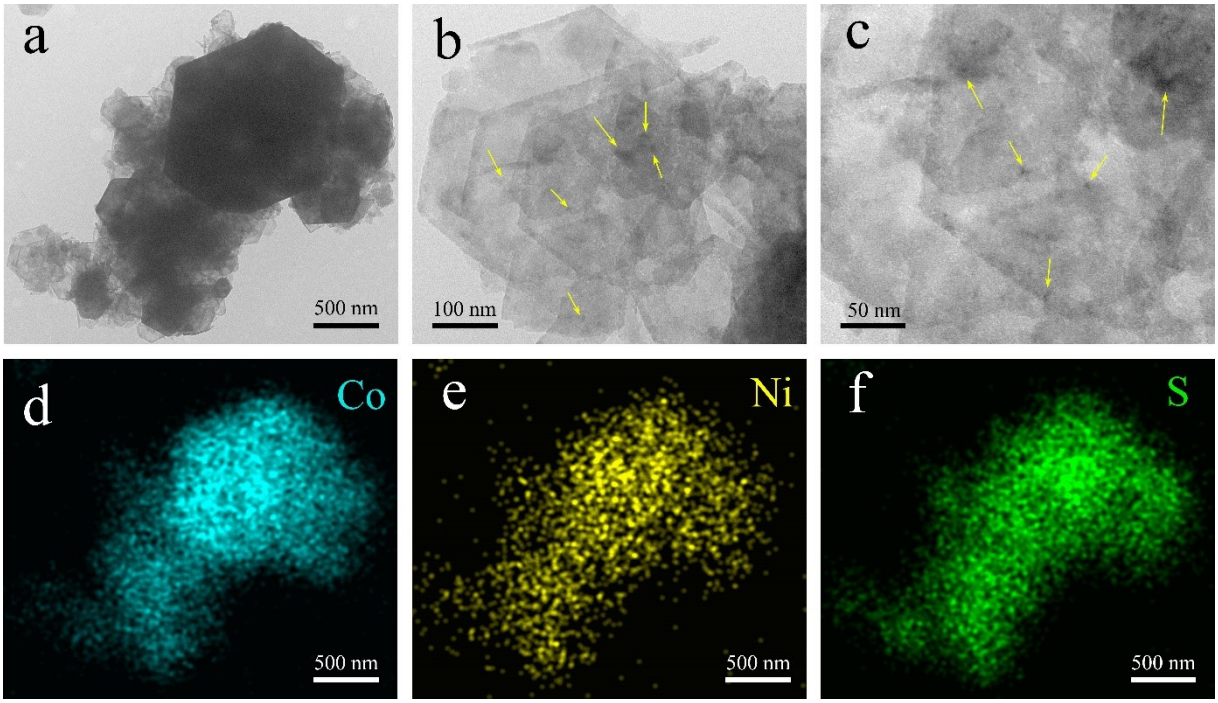

Fig. S4 (a), (b), (c) TEM and elemental mapping of (d) Co, (e) Ni, (f) S in Ni_3S_2/Co_3S_4

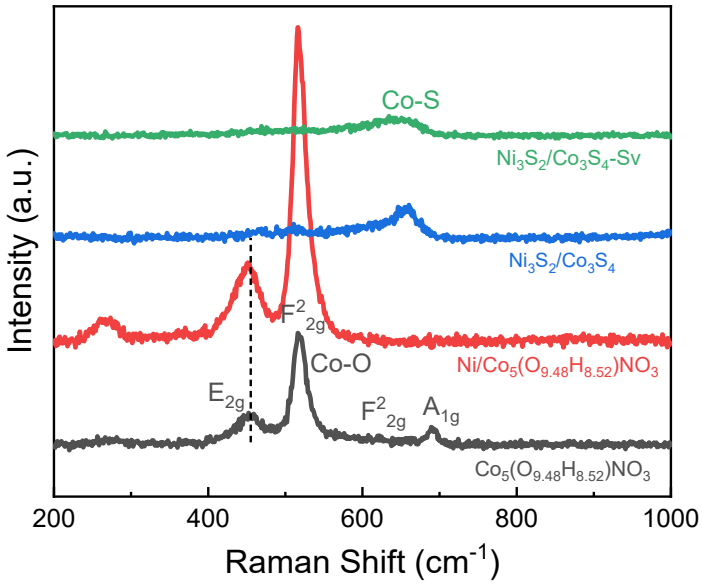

Fig. S5 Raman spectra of samples

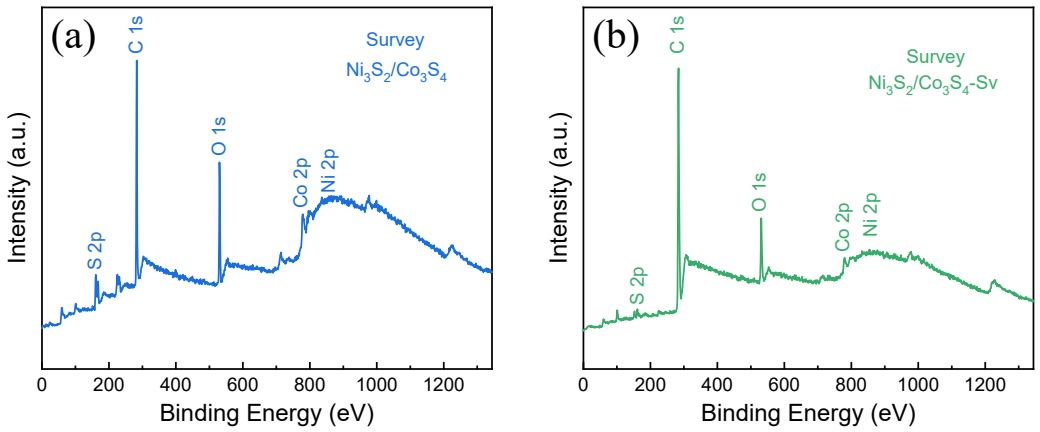

Fig. S6 The survey spectrum of XPS for (a) Ni_3S_2/Co_3S_4, (b) Ni_3S_2/Co_3S_4-Sv

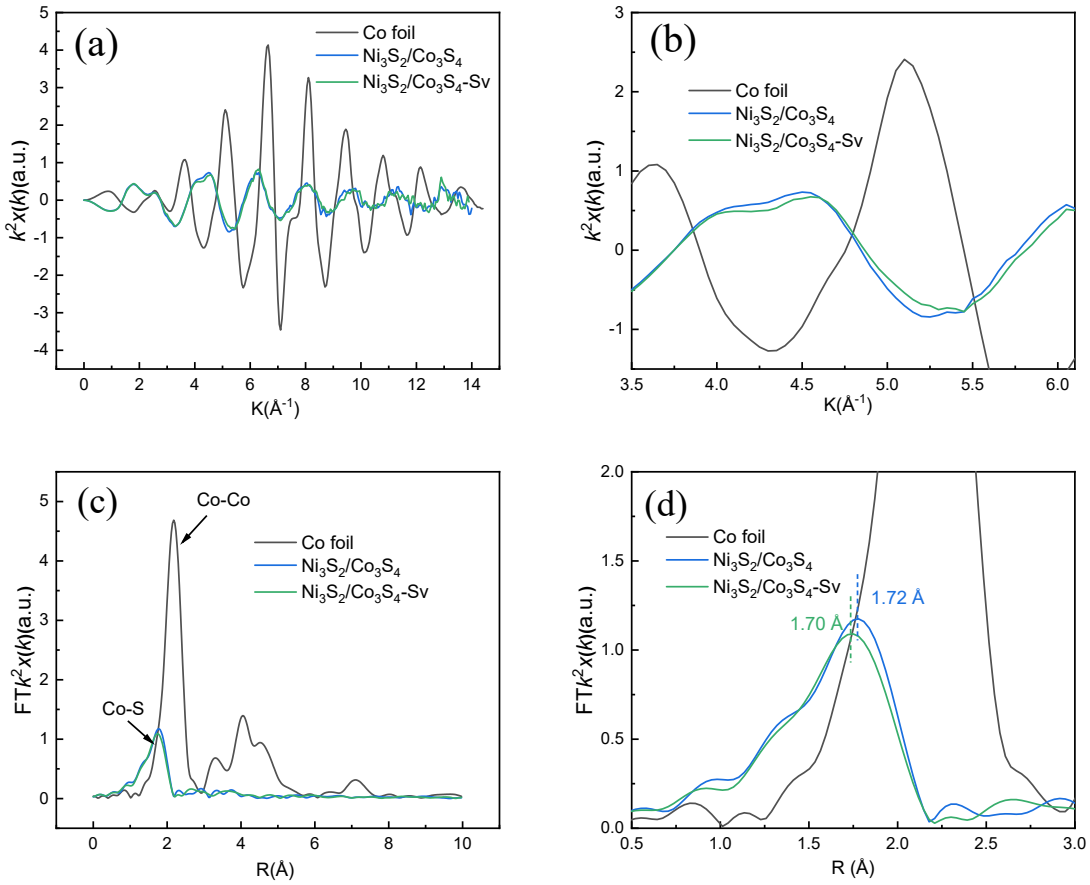

Fig. S7 Co K-edge EXAFS spectra of Ni_3S_2/Co_3S_4 and Ni_3S_2/Co_3S_4-Sv: (a), (b) k-space spectra, (c), (d) R-space

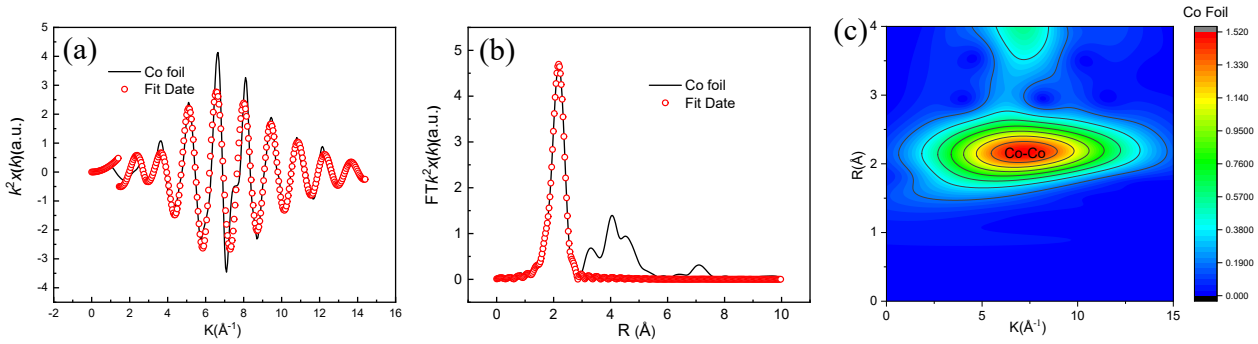

Fig. S8 Co K-edge EXAFS spectra of Co foil: (a) k-space spectra, (b) R-space, (c)

Table S2 EXAFS fitting parameters at the Co K-edge for various samples（S_0^2=0.74）

Sample	shell	CN	R(Å)	σ^2	ΔE_0	R factor
Co foil	Co-Co	12*	2.49±0.01	0.0063	7.6±0.4	0.0021
Ni_3S_2/Co_3S_4-Co	Co-S	3.1±0.1	2.22±0.01	0.0053	-5.0±1.1	0.0091
Ni_3S_2/Co_3S_4-Sv-Co	Co-S	2.8±0.1	2.20±0.01	0.0051	-6.2±1.4	0.0123

Fitting parameters of EXAFS

The obtained XAFS data was processed in Athena (version 0.9.26) for background, pre-edge line and post-edge line calibrations. Then Fourier transformed fitting was carried out in Artemis (version 0.9.26). The k^2 weighting, k-range of 3 - 14 $Å^{-1}$ and R range of 1 - ~3 Å were used for the fitting of Co foil; k-range of 3 - 11.03 $Å^{-1}$ and R range of 1 - ~2.5 Å were used for the fitting of samples. The four parameters, coordination number, bond length, Debye-Waller factor and E_0 shift (CN, R, ΔE_0) were fitted without anyone was fixed, the σ^2 was set.

Parameters for Wavelet Transform analysis

For Wavelet Transform analysis, the χ(k) exported from Athena was imported into the Hama Fortran code. The parameters were listed as follow: R range, 1 - 4 Å, k range, 0 - 15 $Å^{-1}$ for samples; k weight, 2; and Morlet function with κ=10, σ=1 was used as the mother wavelet to provide the overall distribution.

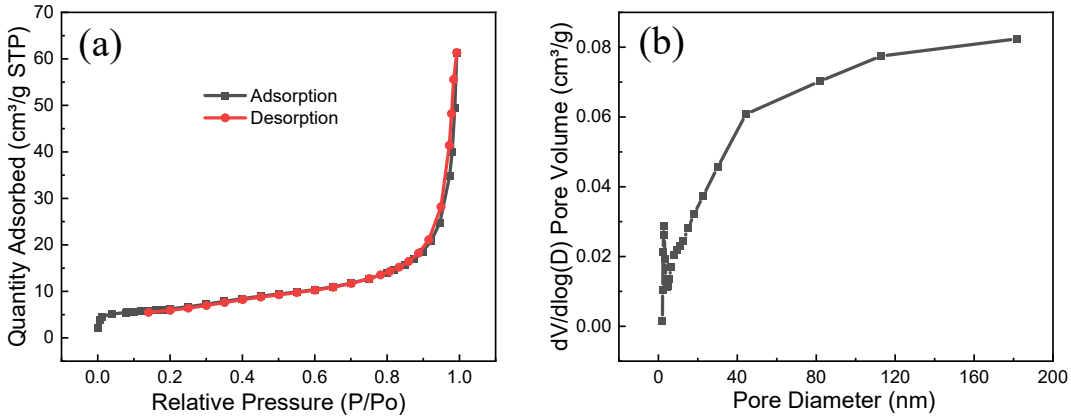

Fig. S9 (a) Nitrogen adsorption-desorption isotherm, (b) BHJ pore size distribution of Ni_3S_2/Co_3S_4-Sv

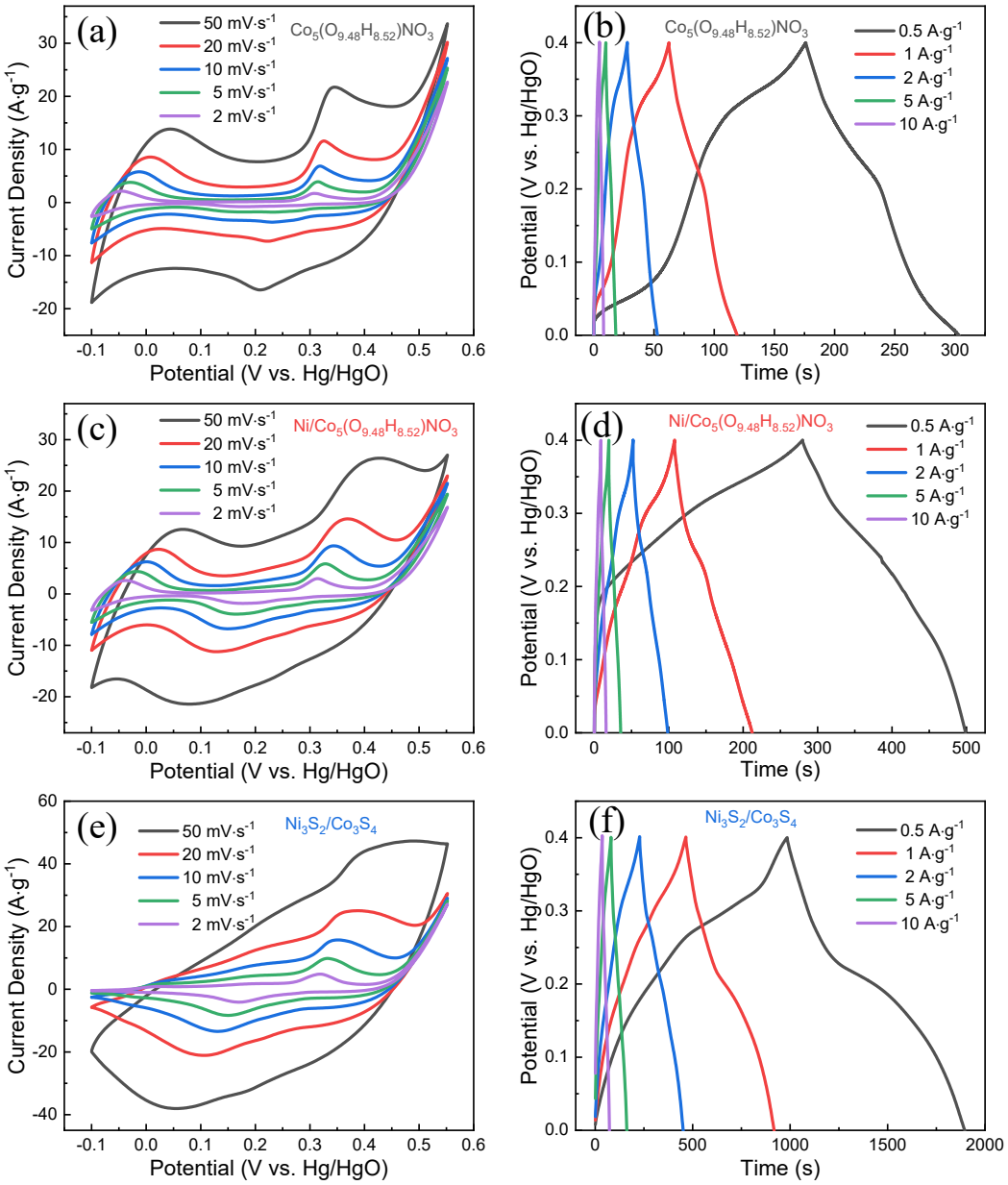

Fig. S10 CV curves at different scan rates of (a) the $Co_5(O_{9.48}H_{8.52})NO_3$ electrode, (c) the $Ni/Co_5(O_{9.48}H_{8.52})NO_3$ electrode, (e) the Ni_3S_2/Co_3S_4 electrode, respectively. GCD profiles at different current densities of (b) the $Co_5(O_{9.48}H_{8.52})NO_3$ electrode, (d) the $Ni/Co_5(O_{9.48}H_{8.52})NO_3$ electrode, (f) the Ni_3S_2/Co_3S_4 electrode, respectively.

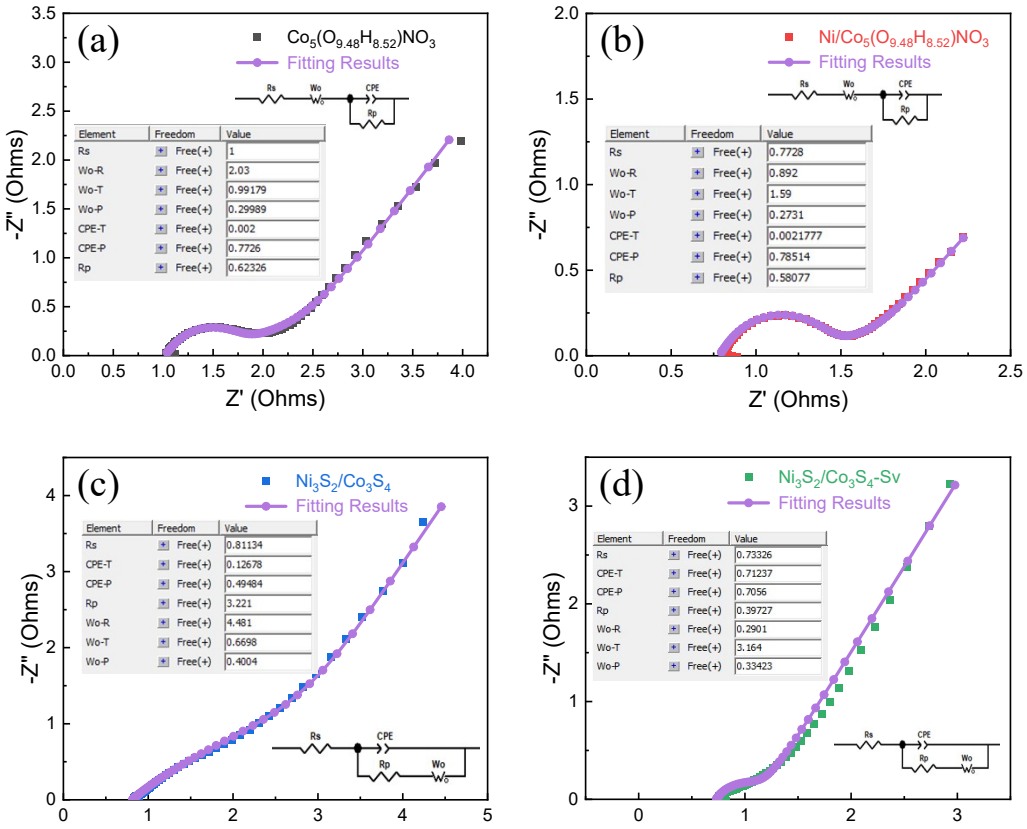

Fig. S11 The EIS fitting results and related equivalent circuit of samples.

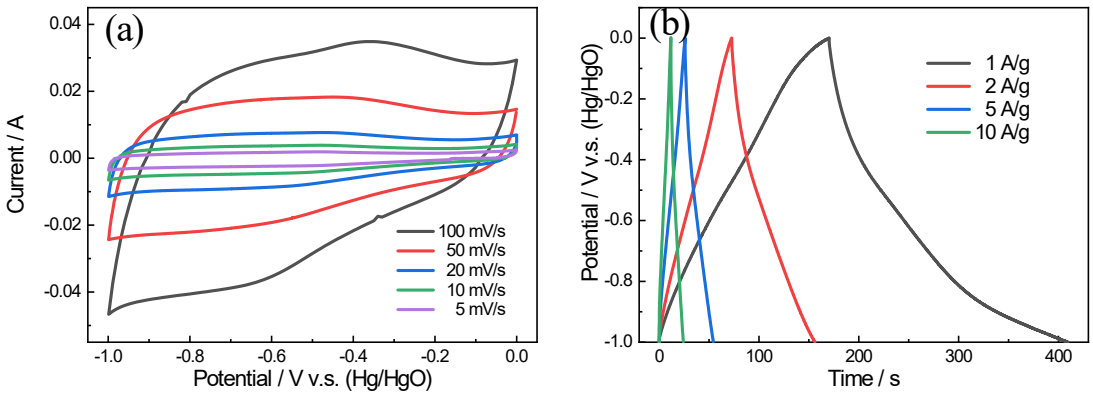

Fig. S12 (a) CV curves at different scan rates and (b) GCD profiles at varied current densities of the AC electrode

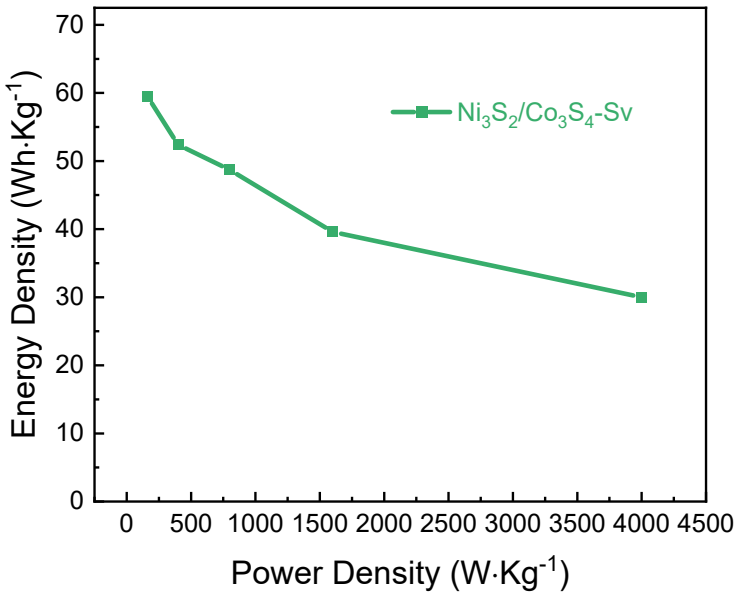

Fig. S13 The energy density vs. power density of Ni_3S_2/Co_3S_4-Sv//AC

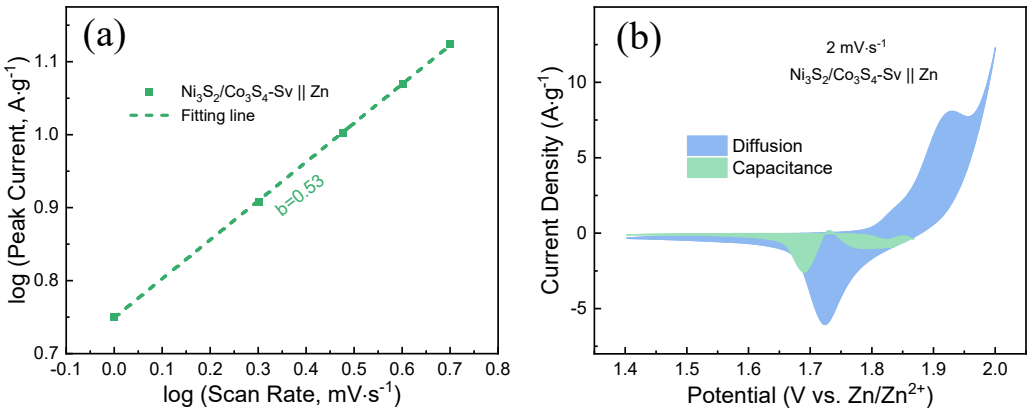

Fig. S14 (a) The plot of peak current vs. scanning rate; (b) Capacitive and diffusion-controlled contribution to charge storage of Ni_3S_2/Co_3S_4-Sv//Zn

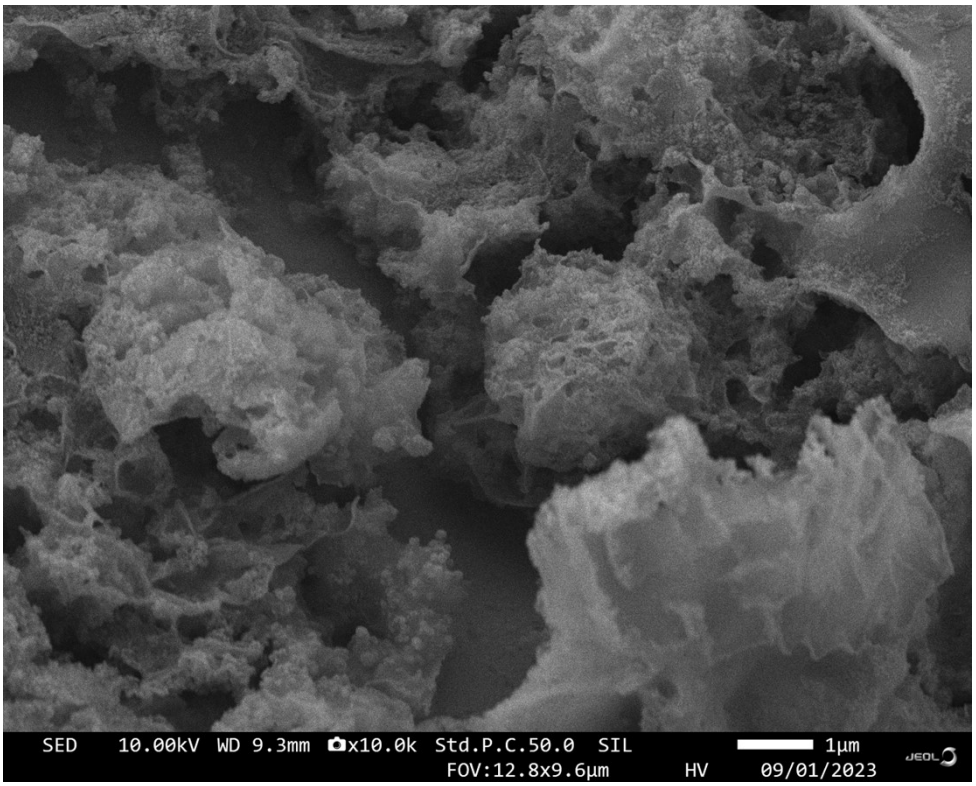

Fig. S15 The SEM image of Ni_3S_2/Co_3S_4-Sv after 2000 cycles

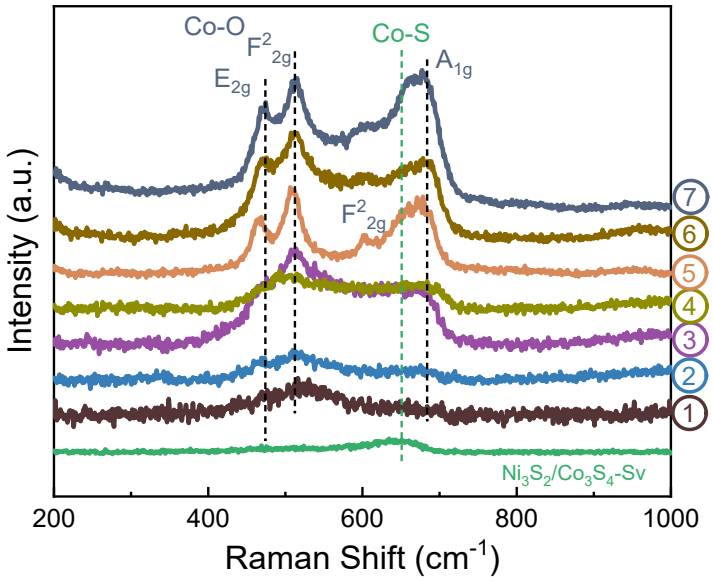

Fig. S16 Ex-situ Raman spectra of Ni_3S_2/Co_3S_4-Sv during charge/discharge process

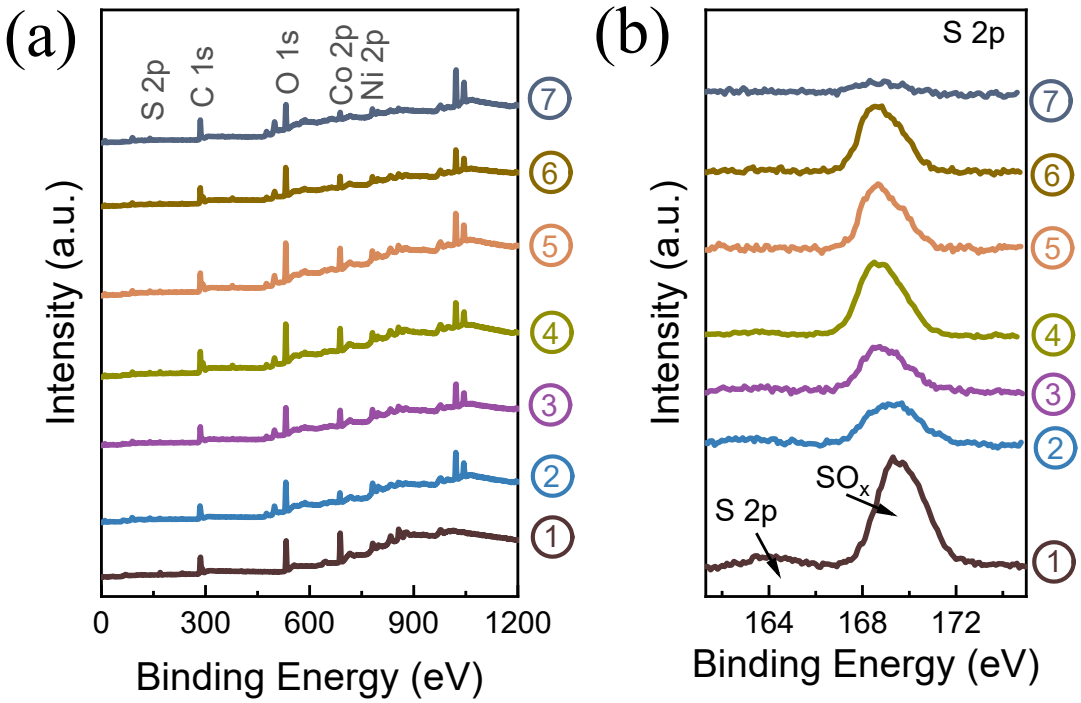

Fig. S17 Ex-situ XPS spectra of (a) survey spectra, (b) S 2p spectra

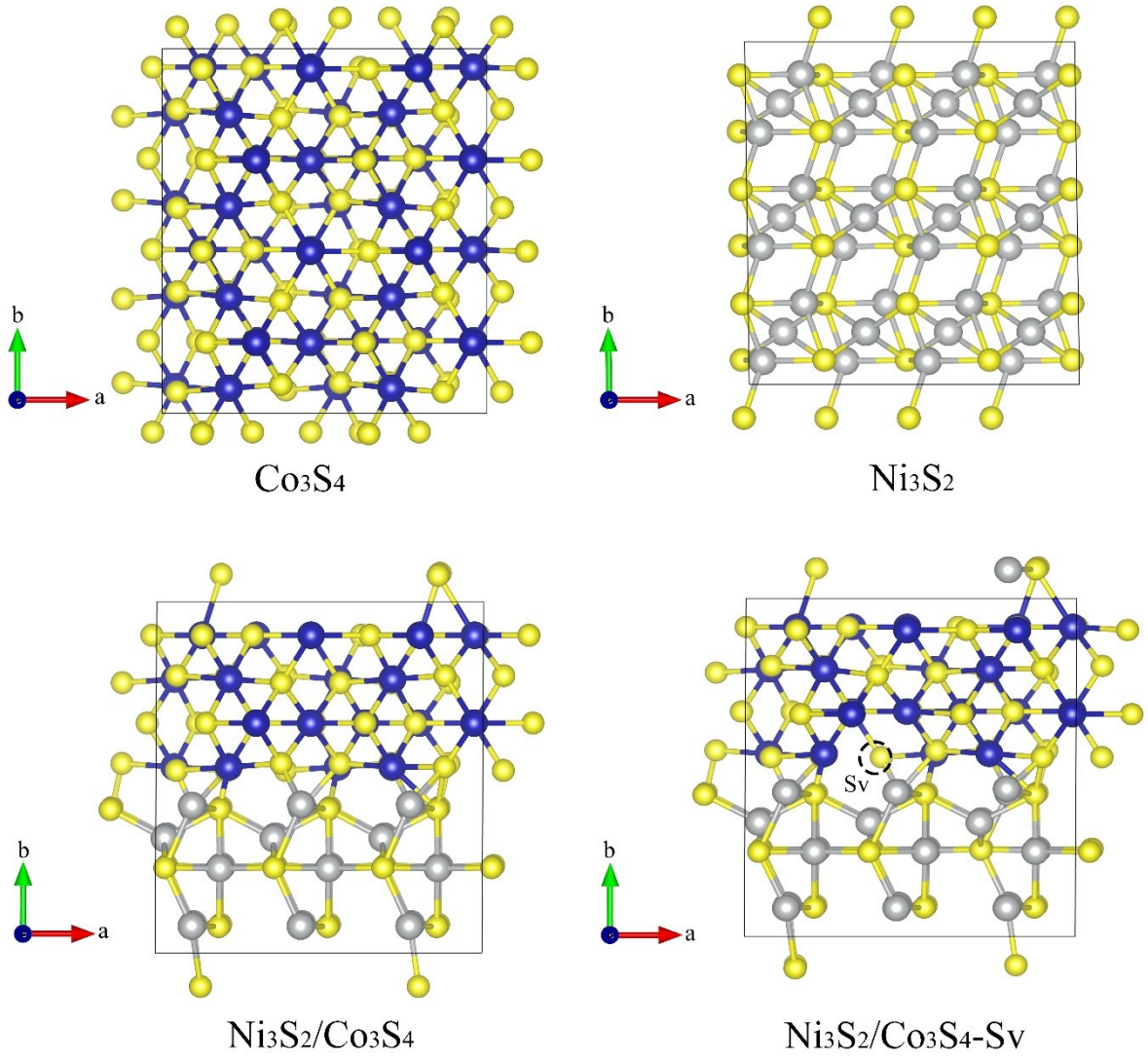

Fig. S18 Top-view models of (a) Co_3S_4, (b) Ni_3S_2/Co_3S_4, (c)Ni_3S_2/Co_3S_4-Sv, respectively.